Electron holography of nanostructured materials

Rafal E Dunin-Borkowski
Center for Electron Nanoscopy, Technical University of Denmark, DK-2800 Kongens Lyngby, Denmark
and Department of Materials Science and Metallurgy, Pembroke Street, Cambridge CB2 3QZ, U.K.

Takeshi Kasama, Edward T. Simpson, Alison C. Twitchett-Harrison, David Cooper and Paul A. Midgley
Department of Materials Science and Metallurgy, Pembroke Street, Cambridge CB2 3QZ, U.K.

Abstract

Three recent examples of the applicaton of off-axis electron holography to the characterization of magnetic and electrostatic fields in nanoscale materials and devices, involving the study of ferromagnetic crystals encapsulated in carbon nanotubes, an assessment of switching reproducibility in patterned spin valve elements and the examination of doped semiconductor device structures in three dimensions using electron holographic tomography, are described.

Introduction

Medium resolution off-axis electron holography is increasingly used to characterize magnetic and electrostatic fields in materials in the transmission electron microscope (TEM) with sub-10-nm spatial resolution. In its standard form, the technique involves applying a positive voltage to an electron biprism in order to overlap a coherent electron wave that has passed through a specimen with a part of the same electron wave that has passed through vacuum. Analysis of the resulting interference pattern allows the phase shift of the specimen wave to be recovered quantitatively and non-invasively. Here, we present three recent applications of the technique and discuss its possible future development.

Methods

The off-axis electron holograms that are presented below were acquired at accelerating voltages of 200 or 300 kV using a Philips CM300ST field emission gun TEM equipped with a 'Lorentz' lens, an electron biprism located close to the conventional selected area aperture plane of the microscope, a Gatan™ imaging filter and a 2048 pixel charge-coupled-device camera. The holograms were acquired with the conventional microscope objective lens switched off and with the specimens located in magnetic-field-free conditions. Reference holograms were used to remove distortions associated with the imaging and recording system of the microscope.

Results

Ferromagnetic iron particles encapsulated in carbon nanotubes

Figure 1 shows a representative experimental result obtained using off-axis electron holography from a 180-nm-diameter carbon nanotube that contains two iron particles, which have dimensions of 36×300 and 11×200 nm and are separated by a distance of 500 nm [1]. The spacing of the magnetic phase contours shown in Fig. 1b, which were obtained using electron holography, is inversely proportional to the in-plane component of the magnetic induction in the specimen projected in the electron beam direction. The contours inside in each particle are not shown. Unwanted contributions to the phase shift, arising from variations in the mean inner potential of the specimen, were removed by using the conventional TEM objective lens to saturate the nanoparticles magnetically parallel and then antiparallel to their long axes. The magnetic contribution to the phase shift was obtained by determining half the difference between phase images that had been acquired with the nanoparticles magnetized in opposite directions, with the microscope objective lens turned off and the sample at remanence. Contours were added to the magnetic contribution to the phase shift to reveal the magnetic flux density in the specimen quantitatively. Figure 1b provides confirmation that both iron particles contain single magnetic domains and shows the characteristic return flux of the larger particle clearly.

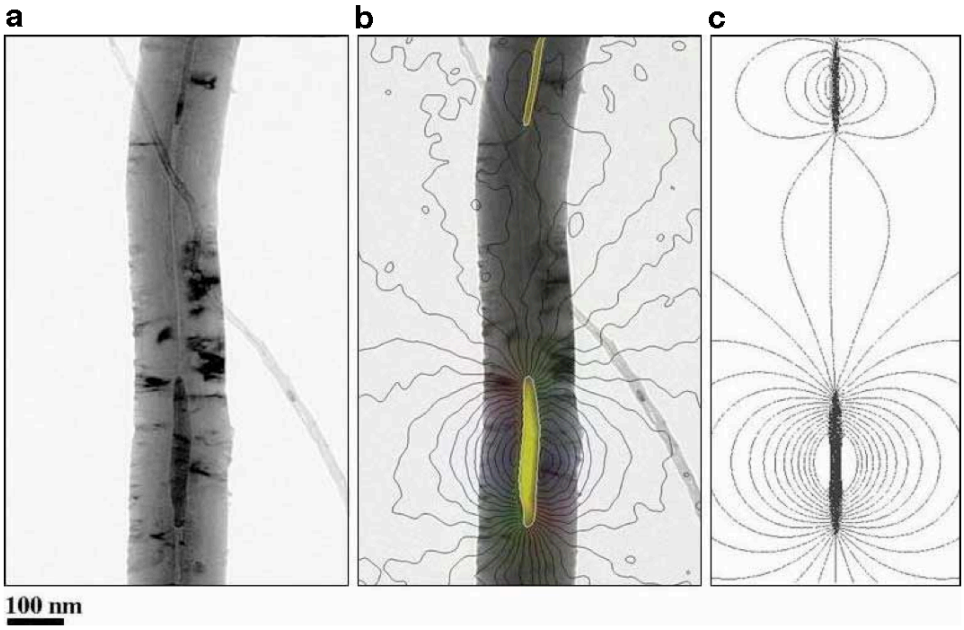

Figure 1. (a) Bright-field TEM image of a multi-walled carbon nanotube, approximately 180nm in diameter, containing 36-nm-diameter and 11-nm-diameter encapsulated iron crystals. (b) Magnetic phase contours, recorded using off-axis electron holography after magnetizing the sample parallel and antiparallel to the direction of the nanotube axis, overlaid onto image (a). (c) Simulated magnetic induction map of two ellipsoidal iron particles with the dimensions and separation of the crystals shown in (a) and (b). The phase contour spacing in (b) and (c) is 0.098 radians.

The micromagnetic simulation shown in Fig. 1c, which was performed for the measured sizes and separation of the particles and the nominal magnetic properties of pure iron, confirms the equilibrium domain state of both particles. The fit to the contours recorded from the smaller particle is poorer, most likely either because its magnetic diameter has been overestimated or because it may contain a larger proportion of carbon than the larger particle, thereby altering its magnetic properties. The quantitative interpretation of the contours is complicated by the fact that their spacing is proportional to the in-plane component of the three-dimensional magnetic induction projected in the electron beam direction. Nevertheless, useful semi-quantitative information about magnetostatic interactions can be obtained by measuring the local contour spacing, or equivalently the gradient of the magnetic contribution to the recorded phase shift.

Pseudo-spin-valve magnetic elements

The preparation of nanoscale magnetic device structures for electron holography is often complicated as a result of the difficulty of preparing an electron-transparent specimen without damaging the magnetic properties of the region of interest on the specimen. A scanning electron micrograph of a magnetic device sample is shown in Fig. 2a. The specimen comprises nominally identical 75×280 nm pseudo-spin-valve elements prepared from polycrystalline $Ni_{79}Fe_{21}$ (4.1 nm)/ Cu (3 nm)/ Co (3.5 nm)/ Cu (4 nm) sputtered onto oxidized silicon. An approach based on focused ion-beam milling with gallium ions, which is described in Fig. 2b, was used to minimize damage to the magnetic properties of the elements during preparation for TEM examination in plan-view geometry. Figure 3 shows six magnetic induction maps of three adjacent elements recorded at remanence using electron holography, after saturating the elements magnetically either parallel or antiparallel to their length using the field of the conventional microscope objective lens, followed by applying a reverse field [2]. These images were used to identify separate switching of the Co and NiFe layers in the individual elements and to measure their switching fields, as shown in the form of a remanent hysteresis loop in Fig. 4.

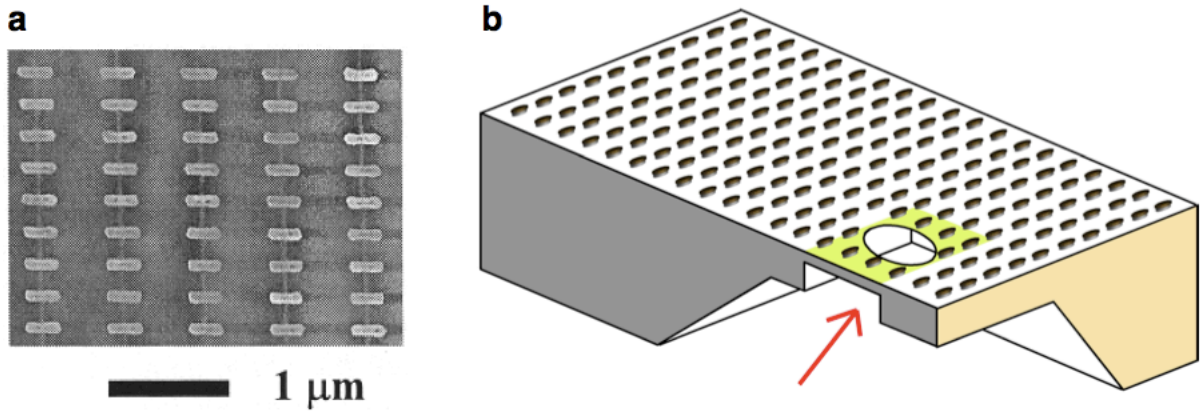

Figure 2 (a) Scanning electron micrograph showing the rectangular array of pseudo-spin-valve elements. (b) Schematic diagram illustrating the final stage of the procedure used to prepare an electron-transparent plan-view sample of the pseudo-spin-valve elements for electron holography, by using focused ion-beam milling with gallium ions. A piece of the wafer is initially milled from the substrate side at one corner. A membrane is formed parallel to the wafer surface. A hole is then formed in this membrane by milling from below, at a glancing angle to the original wafer surface. In this way, the elements that are on the near side of the hole are protected from ion damage and implantation by the intervening substrate, and the hole can subsequently be used to provide a reference wave for electron holography.

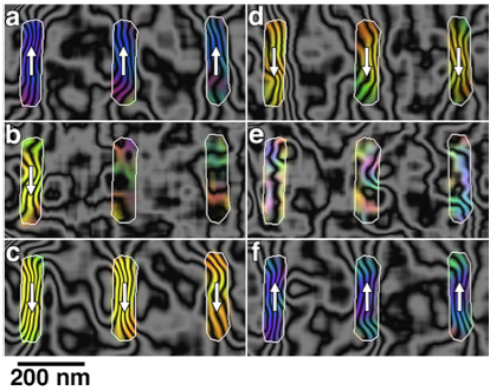

Figure 3 Magnetic induction maps showing six remanent magnetic states recorded using electron holography from three pseudo-spin-valve elements. Eighteen images similar to these were recorded in total. The outlines of the elements are shown in white. The contour spacing is $2\pi/64 = 0.098$ rad, such that the magnetic flux enclosed between adjacent contours is $h/64e = 6.25\text{x}10^{-17}$ Wb. The direction of the induction is shown using arrows and colors (red=right, yellow=down, green=left, and blue=up).

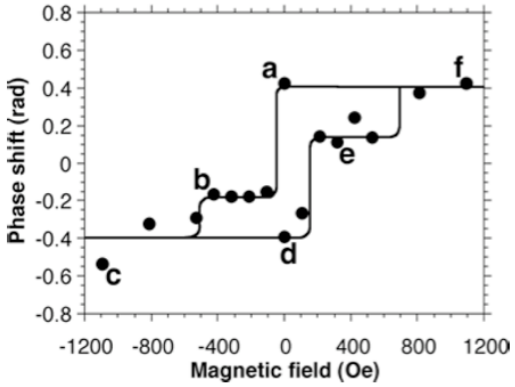

Figure 4 Remanent hysteresis loop measured directly from the experimental electron holographic phase images, with the letters corresponding to the six individual figures shown in Fig. 3. The graph shows the magnetic contribution to the phase shift across each element, plotted as a function of the in-plane component of the field applied to the elements before recording the remanent states. Each point shows an average of the phase shifts measured from the three elements shown in Fig. 3.

A comparison of Fig. 4 with micromagnetic simulations suggests that ~20 nm of material at the edge of each element may not contribute to the magnetic signal, possibly as a result of oxidation or amorphization during fabrication. In addition, the in-plane component of the magnetic induction in the Co layer is reduced by at least 40% from its nominal value. Differences in hysteresis between the three elements are observed, and are thought to result from shape and microstructural variations. This variability must be minimized if such elements are to be used for ultrahigh density recording.

Electron holographic tomography of electrically biased semiconductor devices

The ability to characterize ever smaller device features is of importance for the future development of semiconductor technology. By combining of-axis electron holography with electron tomography, it should be possible to obtain three-dimensional measurements of electrostatic potentials in semiconductor devices. Figures 5a and 5b show a specimen geometry and a specimen holder design that can be used to allow a semiconductor device to be examined under an applied bias using electron tomography and electron holography, as well as allowing the specimen to be transferred to a scanning electron microscope, a focused ion beam workstation or an Ar ion miller in a universal removable cartridge assembly. Figure 5c shows an example of the measured three-dimensional electrostatic potential in a focused ion beam milled Si TEM specimen containing a *p-n* junction, examined under an applied reverse bias voltage of 3 V [3]. Amorphous and crystalline regions contain electrically inactive material at the surfaces of the specimen. Line traces taken across the junction can be used to assess the depletion width and built-in potential across the junction as a function of position in the specimen.

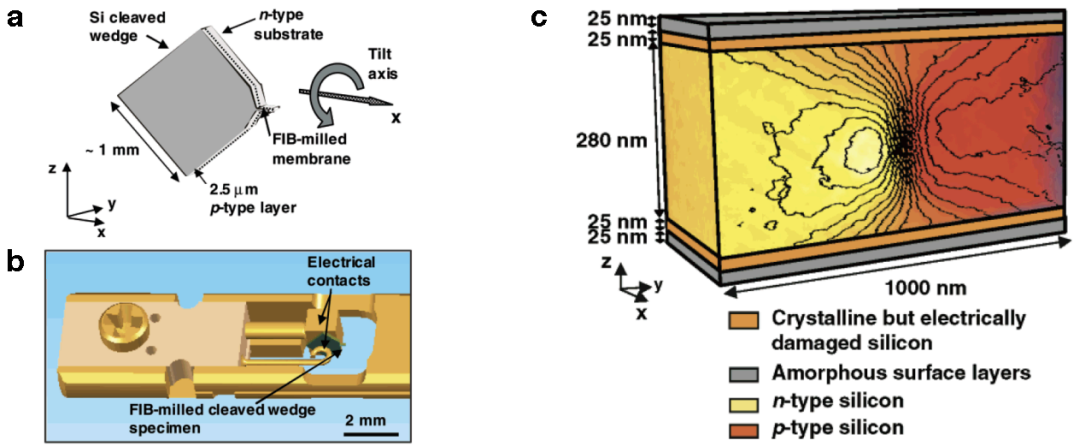

Figure 5. (a) Specimen geometry used for electrically biased tomographic holography. (b) Drawing of a two-contact electrical biasing TEM specimen holder. (c) Tomographic reconstruction of the electrostatic potential in a focused ion beam milled specimen containing an electrically biased Si *p-n* junction. Contours spaced every 0.2 V have been superimposed onto the reconstructed tomogram.

Discussion and Conclusions

Further work is required to optimize specimen preparation for medium resolution electron holography, to increase the sensitivity of the technique for measuring weak fields, to improve its time resolution, and to understand the effect of specimen preparation and electron irradiation on measurements of electrostatic fields. The prospect of characterizing magnetic vector fields *inside* nanocrystals in three dimensions by combining electron tomography with electron holography is also of great interest.

We thank RIKEN, the Royal Society and the EPSRC for support, E.A. Fischione Instruments for holder development, and C.A. Ross, K. Koziol, S.B. Newcomb and T.J.V. Yates for discussions.

[1] K. Koziol, T. Kasama, R.E. Dunin-Borkowski, P. Barpanda and A.H. Windle. Mater. Res. Soc. Symp. Proc. **2006,** 962E, Pittsburgh, PA, 2006, P13.03.

[2] T. Kasama, P. Barpanda, R.E. Dunin-Borkowski, S.B. Newcomb, M.R. McCartney, F.J. Castano and C.A. Ross, J. Appl. Phys. 98 (2005) 013903.

[3] A.C. Twitchett, T.J.V .Yates, S.B. Newcomb, R.E. Dunin-Borkowski and P.A. Midgley, Nano Letters **7** (2007), 2020-2023.